P-ISSN 2586-9000
E-ISSN 2586-9027
Homepage : https://tci-thaijo.org/index.php/SciTechAsia
Science & Technology Asia
Vol.26 No.4 October - December 2021
Page: [13-26]
Original research article

Effect of Suction/Injection on the Stream of a Magnetohydrodynamic Casson Fluid over a Vertical Stretching Surface Installed in a Porous Medium with a Variable Heat Sink/Source

Ravindra Kumar[1,2], Ruchika Mehta[1,*], Kalpna Sharma[1], Devendra Kumar[3]

[1]*Department of Mathematics & Statistics, Manipal University Jaipur, Jaipur 303007, India*
[2]*Department of Mathematics, Vivekananda Global University, Jaipur 303012, India*
[3]*Department of Mathematics, University of Rajasthan, Jaipur 302004, India*

Received 08 August 2021; Received in revised form 24 November 2021;
Accepted 27 November 2021; Available online 30 December 2021

ABSTRACT

In this paper, we examined the heat transmission properties of a 2D magnetohydrodynamic stationary Casson shear thickening liquid via a perpendicular extending pane installed in a permeable medium in the existence of a changeable warmth sink/source. The effect of current energy is also measured. With appropriate likeness changes, the leading partial differential equations and agreeing borderline circumstances are transported to ordinary equations and answered numerically by the Runge-Kutta fourth-order methods with shooting procedure. Concurrent results to the event of injection and suction are presented. The encouragement of various non-dimensional factors on velocity and temperature circulations with skin friction factor and resident Nusselt numeral was analyzed by graphs and tables for both injection and suction belongings. Growth in magnetic field limits primes to diminution in velocity and improve the circulation of temperature. Biot numeral and radiation limit help to rise the velocity field and circulation of temperature field in both the cases injection and suction. Nusselt numeral is lessened for an appreciation for the values of magnetic arena, Biot numeral, Prandtl numeral, Permeability restriction, Eckert numeral and non-unchanging heat sink/source restrictions (A^*, B^*) and increased for Grashof numeral. Friction factor is a growing function of Grashof numeral, Eckert numeral and non-unchanging heat sink/source restrictions (A^*, B^*) and decreased for magnetic field, Biot numeral, Prandtl numeral, Permeability restriction.

***Corresponding author:** ruchika.mehta1981@gmail.com

Keywords: Casson fluid; Extending surface; Heat source/sink; Permeability; Suction/injection

1. Nomenclature

(u,v) are the velocity components in the ways (x,y), correspondingly.

v is the viscosity.

T is the fluid temperature.

T_∞ is far away temperature.

σ is the electric conduction.

k is the thermal conduction.

g is acceleration due to gravity.

ρ is the fluid density.

β is Casson fluid restriction.

C_p is the heat capacity.

q''' is the flexible heat sink or source.

q_r is radiative heat flux.

k^* mean absorption coefficient.

r^* Stefan–Boltzmann constant.

L is the molecular permitted mean route.

v_w is the suction velocity.

h_f is the convective heat transport.

Gr is the Grashof numeral.

M is the magnetic field restriction.

Ra is the radiation restriction.

Pr is the Prandtl numeral.

S is the suction/injection restriction.

γ is the first-order velocity slip restriction.

K is porous medium permeability.

Ec is the Eckert numeral.

Bi is the Biot numeral.

C_{f_x} is the skin friction constant.

Nu is the local Nusselt numeral.

Re_x is the local Reynolds numeral.

p_y is the yield stress of the fluid.

μ_B is the plastic dynamic viscosity of Casson fluid.

2. Overview

Non-Newtonian fluids mean areas of propagation and research for enthusiastic benefits in medicine, engineering, industry, and mathematics. Many models are considered due to the non-linear relationship between stress and deformation rate. Non-Newtonian fluids have innumerable instances in everyday life, such as fabric softener production, food storage, newspaper production, and dissimilar lubricant performance. On Newtonians is inherently complex due to its complexity. Investigating a single model that represents all of its characteristics can be a daunting task. Hayat and Alsaedi [1] explored the belongings of frictional and Thermic heat on the MHD motion of Oldroyd-B shear deepening fluids on overextended sheets. Zheng and jin [2] intentional the time reliant on movement of MHD on a non-constant stretched sheet with thermal diffusion. The time-reliant on allowed convection transfer of the MHD Casson liquid crossways the permeable pane was explored by Khalid and khan [3]. Ready [4] examine the unsteady 2-dimensional stream of non-Newtonian fluids on stretched surfaces with the belongings of current radiation and adjustable current conduction is explored. The Casson fluid perfect is used to illustrate the behavior of non-Newtonian fluids. Hayat and Asad [5] talked the belongings of non- unchanging warmth sinks/sources and heat energy on the stream of coupled stress fluids by extension cylinders in a thermo stratification medium. Kataria and Patel [6] discussed the conclusion of warmth generation on the stream of MHD Casson fluid in a absorbent medium. Recently, Kataria and Patel [7] deliberate the belongings of chemical reactions on MHD problems in porous media. Sandeep and Korkiko [8] measured kinematic viscosities whereas learning the stream of 3-dimensional Casson fluids. The heat transfer properties of the stable 2-dimensional boundary laminar stream of an

incompressible electrically conductive Casson fluid passing through a revolving plate in the existence of a absorbent medium were debated by Raju and Sandeep [9]. Naramgari and Sulochana [10] described the effects of chemical reactions and radioactivity on the stable incompressible 2D MHD stream through a absorbent surface during suction/injection. Ahmad et al. [11] intentional a stationary 2D MHD shear concentrate on wedges heated by Newtonian. Arifuzzaman and Hossain. [12] EFDM analysis and convergence and stability experiments were performed. Baagand Mishra [13] conversed the steady 2D motion of an incompressible magnetic micropolar fluid in a region of stagnant stream on a plate vertically heated by a chemical reaction. Kumaran and Sandeep [14] measured the parabolical stream of MHD Casson fluids. Khan and Waqas [15] discovered MHD Casson fluid inaction argument stream with the reaction of standardized heterogeneous belongings. Tamoor and Waqas [16] explored the Newtonian boiler properties of the MHD Casson liquid stream originated by a overextended cylinder moving at lined velocity. Hussananand Salleh [17] considers the stable 2-dimensional stream of a viscous Casson fluid through the expansion surface below the influence of current energy and viscous debauchery. Ullah and Shafie [18] premeditated the belongings of Brownian and thermophoresis gesture on MHD stream with changed geometries. Kumar and Sugunamma [19] Examine the motion of a non-associated radiative inaction point of a non-Newtonian fluid (MHD) concluded an extended pane. Mohyud-Din and Usman [20] discuss Semi-analytical solution for warmth transmission investigation of fondling stream of Casson fluid among corresponding rounded dishes. Animasaun and Koriko [21] offered a numerical explanation to the borderline coating stream problem of nanofluidic streams across a dense surface with Hall belongings. Doganchi et al. [22] investigated the part of expected convection and current radioactivity in the thermo-hydrodynamics dynamics of nanofluid warmth transmission in a loop amongst a rounded undulating cylinder and a rhombic container subjected to an unchanging magnetic arena. A new model of viscidness called magnetic field dependent viscosity (MFD) was used. Doganchiand Ismael [23] presents a numerical investigation of the convection of a water-based, copper-based nanofluid that fills a trilateral void with a hemispherical bottom wall. Doganchi and Armaghani [24] See ordinary convection in a crater containing an elliptical inclined boiler under the form influence of nanoparticles and magnetic arena Doganchi and Sheremet [25]. The usual convection warmth transmission of copper nanofluid and water in a absorbent gap amongst the hot inward four-sided tube and the cold outside rounded pipe over the encouragement of the uniform persuaded magnetic arena has been explored. Kumar and Ramadevi [26] premeditated the current properties of a stable incompressible MHD stream of Powell-Eyring liquid because of section contraction with non-uniform warmth restrictions. Kumar and Reddy [27] The belongings of warmth and mass transmission on both the time-reliant on and time- reliant not on MHD stream of the Williamson liquid because of the curled surface are discoursed. Kumar and Reddy [28] gave twin explanations of the MHD stream of Williamson's liquid on a curled pane. Visualize that the movement of fluids depends on class and time. Kumar and Sugunamma [29] studied the conclusion of Arrhenius initiation energy on the varied convective inaction point stream of magneto-hydrodynamic micro-electrode fluid done an adjustable thick surface in the presence of Brownian motion. Kumar and Sugunamma [30] carry a numerical learning of the electrically leading nonlinear MHD convective stream of a polar microfluid on a

slandering stretching surface. Reza-E-Rabbi and Arifuzzaman [31] study conveyed an unambiguous limited variance on the stream of unstable, chemically reactive Cason-type fluids using MHD and an expansion plate. They also included Brownian dispersal and thermophoresis in this study. Agrawal and Dadheech [32-33] discuss the Radiative MHD hybrid nano fluids stream and Magneto marangonimovement of γ-al2o3 nano fluids above a holey extending surface with warmth sink/source fixed in permeable medium. Mathur Mishra [34] describes the Entropy generation in a micropolar liquid past an inclined channel with velocity slip and warmth flux circumstances. Dadheech and Agrawal [35] give the Entropy study for radiative inclined MHD slip stream with warmth source in permeable medium for two unlike liquids.

3. Mathematical Formulations

Deliberate a 2D normal convective stream of an incompressible non-Newtonian Casson fluid that conducts electricity over a upright surface in the existence of velocity slip. The stream is laminar and constant. The impact of the magnetic Reynolds numeral and the persuaded magnetic field is unnoticed. The effects of thermal radiation and flexible heat sinks/sources are observed. The convective boundary state is active to the border. It is certain that the surface extending with a velocity $u_w(x) = ax$ in the x path is shown in Fig. 1, where a is the preliminary extending rate. A continual magnetic force field of asset $B = B_0$ is applied in the reverse path. The rheologic equation of state for the Cauchy stress tensor of Casson fluid can be written as

$$\tau_{ij} = \begin{cases} 2\left(\mu_B + \dfrac{P_y}{\sqrt{2\pi}}\right)e_{ij}, & \pi > \pi_c, \\ 2\left(\mu_B + \dfrac{P_y}{\sqrt{2\pi_c}}\right)e_{ij}, & \pi < \pi_c, \end{cases}$$

where $\pi = e_{ij}e_{ji}, e_{ij}$ is the $(i,j)^{th}$ factor of the distortion rate with itself, π_c is the critical value of this product created on the shear thickening model, μ_B is the plastic dynamic viscosity of Casson fluid, and p_y is the yield stress of the fluid.

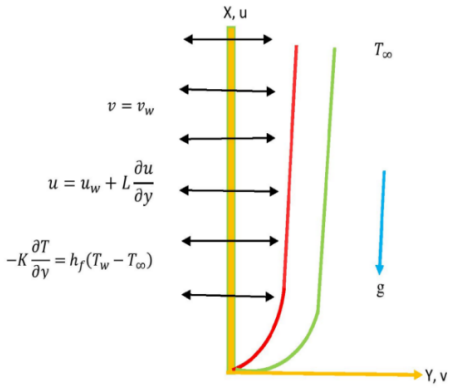

Fig. 1. Stream geometry.

Equation of Continuity

$$\frac{\partial u}{\partial x} + \frac{\partial v}{\partial y} = 0, \tag{3.1}$$

Equation of Momentum

$$u\frac{\partial u}{\partial x} + v\frac{\partial u}{\partial y} = v\left(1 + \frac{1}{\beta}\right)\frac{\partial^2 u}{\partial y^2} - \frac{\sigma}{\rho}B_0^2 u + g\beta(T - T_\infty) - \frac{v}{K}\left(1 + \frac{1}{\beta}\right)u, \tag{3.2}$$

Equation of Energy

$$u\frac{\partial T}{\partial x} + v\frac{\partial T}{\partial y} = \frac{k}{\rho C_p}\frac{\partial^2 T}{\partial y^2} + \frac{q'''}{\rho C_p} - \frac{1}{\rho C_p}\frac{\partial q_r}{\partial y} + \frac{\sigma}{\rho C_p}B_0^2 u^2 + \frac{v}{C_p}\left(1 + \frac{1}{\beta}\right)\left(\frac{\partial u}{\partial y}\right)^2, \tag{3.3}$$

everywhere (u, v) are the velocity components in the ways (x, y), correspondingly, υ is the viscosity, T is the fluid temperature, far away temperature is T_∞, σ is the electric conduction, k is the thermal conduction. g is acceleration due

to gravity. The fluid density is ρ, Casson fluid restriction is β, C_p is the heat capacity, the flexible heat sink or source is q''', and radiative heat flux is q_r. q''' is plus to deliberate the thought of variable heat sink or source, and it is given by

$$q''' = \frac{ku_w}{xv}\left(A^*\left(T_w - T_\infty\right)\right)f' + B^*\left(T - T_\infty\right), \tag{3.4}$$

Here, $\left(T_w - T_\infty\right) = bx$, where T_w is the temperature adjacent to the walls. By the Rosseland's estimate, the radiative heat flux is

$$q_r = -\frac{4}{3}\frac{\sigma^*}{k^*}\frac{\partial T^4}{\partial y}, \tag{3.5}$$

where k^* and σ^* are mean absorption coefficient and the Stefan-Boltzmann constant, correspondingly. The expansion of Tailor series of T^4 about T_∞ is

$$T^4 = 4TT_\infty^3 - 3T_\infty^4. \tag{3.6}$$

For present study the boundary conditions are

$$u = u_w + L\frac{\partial u}{\partial y}, v = v_w - k\frac{\partial T}{\partial y} = h_f\left(\left(T_w - T_\infty\right)\right),$$
$$\text{at } y = 0, u \to 0, T \to T_\infty \text{ as } y \to \infty, \tag{3.7}$$

where the molecular permitted mean route is L, the suction velocity is v_w and the convective heat transport is h_f. If $v_w(x) < 0$, we have an injection and $v_w(x) > 0$, we have suction.

4. Mathematical Process for Result

To translate equations (3.1-3.3) into a set of ODEs, the succeeding likeness renovations and non-dimensional variables are introduced. Let us express the likeness variable η as

$$\eta = \sqrt{\frac{a}{v}}y. \tag{4.1}$$

Let us describe the components of velocity in relations of stream function ψ as

$$\psi = \sqrt{av}xf(\eta), u = \frac{\partial\psi}{\partial y} = axf'(\eta),$$
$$v = -\frac{\partial\psi}{\partial x} = -\sqrt{av}f(\eta), \theta(\eta) = \frac{T - T_\infty}{T_w - T_\infty}, \tag{4.2}$$

where ψ, η are the stream function and likeness variable, and $\theta(\eta), f'(\eta)$ are the dimensionless forms of temperature and velocity of the fluid. With equation (4.1) and (4.2), the equation of continuity is fulfilled trivially and Eqs. (3.2) and (3.3) convert as.

$$\left(1 + \frac{1}{\beta}\right)f''' + ff'' - f'^2 - \left(M + \left(1 + \frac{1}{\beta}\right)K\right)f' + Gr\theta = 0, \tag{104.3}$$

$$(1 + Ra)\theta'' + \left(A^*f' + B^*\theta\right) + Pr\left(f\theta' - f'\theta + ME_cf'^2 + \left(1 + \frac{1}{\beta}E_cf''^2\right)\right) = 0, \tag{4.4}$$

where $Gr = \frac{g\beta\left(T_w - T_\infty\right)}{a^2x}$ is the Grashof numeral, $M = \frac{\sigma B_0^2}{a\rho}$ is the magnetic field restriction, $Ra = \frac{16\sigma^*T_\infty^3}{3kk^*}$ is the radiation restriction, $Pr = \frac{v\rho C_p}{k} = \frac{\mu C_p}{k}$ is the Prandtl numeral, $S = -\frac{v_w}{\sqrt{av}}$ is the suction/injection restriction, and $\gamma = L\sqrt{\frac{a}{v}}$ is the first-order velocity slip restriction, $K = \frac{v}{ak}$ is porous

medium permeability restriction, $Ec = \frac{ax}{C_p}$ is the Eckert numeral. The agreeing boundary conditions are

$$f' = 1 + \gamma f'', f = S, \theta'(0) = -Bi(1 - \theta(0)), \text{ at } \eta = 0, \quad (4.5)$$

$$f'(\eta) \to 0, \theta(\eta) \to 0 \text{ as } \eta \to \infty, \quad (4.6)$$

where $Bi = \sqrt{\frac{v}{a}} \frac{h_f}{k}$ is the Biot numeral.

The skin friction constant C_{f_x} and local Nusselt numeral Nu.physical quantities are specified by:

$$C_{f_x} Re_x^{\frac{1}{2}} = \left(1 + \frac{1}{\beta}\right) f''(0), \quad (4.7)$$

$$NuRe_x^{-\frac{1}{2}} = -(1 + Ra)\theta'(0), \quad (4.8)$$

where $Re_x = \frac{xu_w}{v}$ (4.9)

is the local Reynolds numeral The result of Eqs. (4.3-4.4) jointly through borderline circumstances (4.5-4.6) is determine through by a systematic numerical method be aware shooting technique. We translate the nonlinear equivalences into first order regular differential equivalences by labelling the variable quantity i.e.

$$f = f_1, f' = f_2, f'' = f_3, f''' = f_3', \\ \theta = f_4, \theta' = f_5, \theta'' = f_5', \quad (4.10)$$

Hence, the system of equations becomes

$$f_1' = f_2, f_2' = f_3, f_3' = \left(1 + \beta^{-1}\right)^{-1} \left[f_2^2 - f_1 f_3 - Grf_4 + \left(M + K\left(1 + \beta^{-1}\right)\right) f_2 \right], f_4' = f_5, \quad (4.11)$$

$$f_5' = (1 + Ra)^{-1} \left[Pr(f_2 f_4 - f_1 f_5 - ME_c f_2^2 - E_c \left(1 + \beta^{-1}\right)^{-1} f_3^2) - \left(A^* f_2 + B^* f_4\right) \right], \quad (4.12)$$

subject to the subsequent conditions

$$f_1(0) = S, f_2(0) = 1 + \gamma S_1, f_3(0) = S_1, \\ f_4(0) = 1 + Bi^{-1} S_2, f_5(0) = S_2 \text{ as } \eta \to 0 \text{ and } \\ f_2(\infty) = 0, f_4(\infty) = 0 \text{ as } \eta \to \infty. \quad (4.13)$$

Now fourth order Runge-Kutta way with shooting technique is follow for stepwise integration and calculations are passed out on MATLAB computer software.

5. Outcomes and Discussion

Adjustment Nonlinear ordinary differential Eqs. (4.3-4.4) with limit (4.5-4.6) were resolved by the shooting and Runge - Kutta way of fourth order with MATLAB package. The outcomes got display the influence of non-dimensional rule limits, regarding friction factor, Nusselt values, velocity and temperature, studied in full and displayed through tables and graphs. Figs. 2 and 3 show the effect of suction/injection restriction (S) on velocity and temperature. The design lets us to achieve that the velocity and temperature fields reducing through the suction/injection restriction. By put on suction it carries the sum of liquid elements to the wall. Later, the impetus coat depth and thermal limit are reduced by the suction/injection restriction. The magnetic field (M) limitation effect on the velocity and temperature field deliveries is exposed in Figs. 4 and 5. Note that growing the number of M results in a diminution in the velocity field. Increase in the limits of the magnetic field results in a kind of resistive called the Lorentz force created in the stream that reasons a diminution in the curve in the velocity field. It is noted that growth in the magnetic limit growths the temperature circulation. Because of the Lorentz force, some warmth will be created in the stream. The intensification in the magnetic field suppresses the momentum thickness and growths the thermal coating depth. Fig. 6 delineated to get the act of Casson fluid

restriction (β) on the transfers of velocity. Fig. 6, we observed that the improvement in Casson fluid restriction lessens the circulation of velocity and the matching borderline coating width. Fig. 7 and 8 exhibits the significance of the radiation restriction Ra on the distributions of velocity and temperature, respectively. It is vibrant as of the Figs. 7 and 8 that the intensification in radiation restriction upsurges the fluid velocity and temperature. Heightening in radiation of restriction releases warmth energy to the stream so this energy supports to increase in value the velocity and temperature arena. Fig. 9 is depicted the import of unequal sink/source restrictions $A*$ on thermal arenas. It is apparent as of the figure that the intensification in $A*$ upsurges the temperature arenas. Enhancing the unequal warmth restrictions progresses the temperature and coating width. It is weighty that a higher temperature is attained in the situation of injection likened to case of suction. Fig. 10 is depicted the significance of unequal sink/source restrictions $B*$ on velocity. Intensification in $B*$ decreases the velocity. Figs. 11 and 12 labels the stimulus of Biot numeral on velocity and temperature arena. As of the figure, we perceived that velocity and temperature are a rising function of Biot numeral. Fig. 13 shows that as permeability restriction K increases, fluid temperature increase. Fig. 14 shows the circulations of temperature for modification in the thermal Grashof numeral. From Fig. 14, the circulation of temperature is the lessening function of Gr. Because of higher buoyancy services, the liquid temperature will be declaimed. Hence, lessening in thermal arena are detected with an intensification in Gr. The impact of Prandtl numeral Pr on the circulation of velocity and temperature arena is exposed in Figs. 15 and 16. It is perceived that growing of Pr results an abatement in velocity and temperature arena. The impact of Eckert numeral Ec on the circulation of velocity and temperature arena is exposed in Figs. 17 and 18. It is perceived that growing of Ec results an abatement in velocity and temperature arena. The disparity of skin friction factor and the rate of thermal transmission for unlike values of physical restrictions $M, Bi, Pr, K, Gr, A^*, B^*, Ec, \beta$ and Ra have been exposed in the table 1. As of the table, we recognize the subsequent outcomes. Strengthening in the value of M, Bi, Pr and K marks a abatement in the friction factor and warmth transmission rate for both cases. Intensification in the value of Gr result an increment in the friction factor and heat transfer rate for both cases. Intensification in the value of A^*, B^* and Ec boost the factor of skin friction, but a contrary tendency is perceived for local Nusselt numeral.

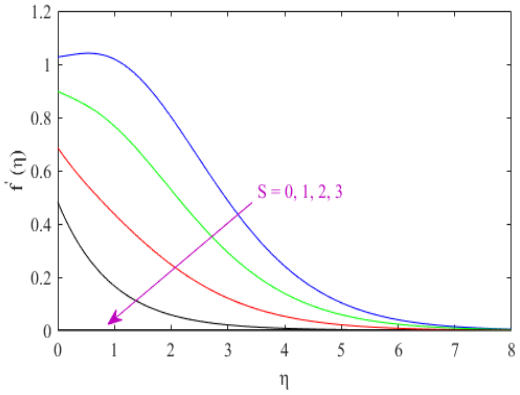

Fig. 2. Velocity profiles $f'(\eta)$ against η for unlike facts of suction/injection restriction S.

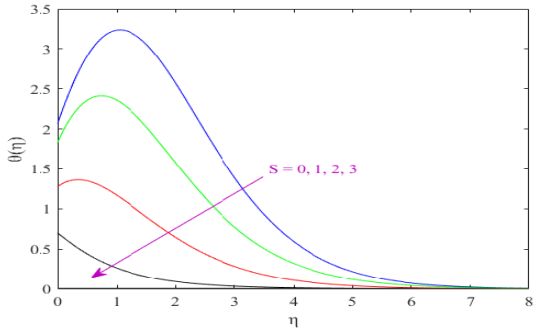

Fig. 3. Temperature $\theta(\eta)$ against η for unlike facts of suction/injection restriction S.

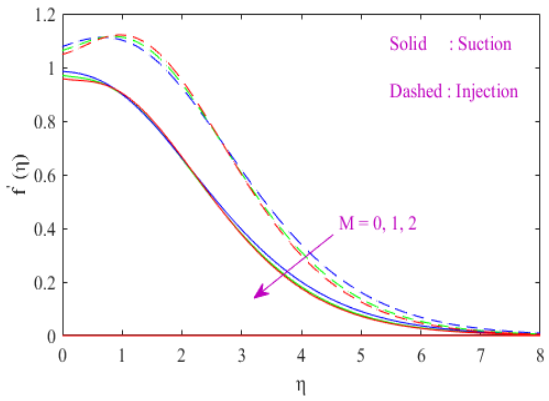

Fig. 4. Velocity $f'(\eta)$ against η for unlike facts of Magnetic restriction M .

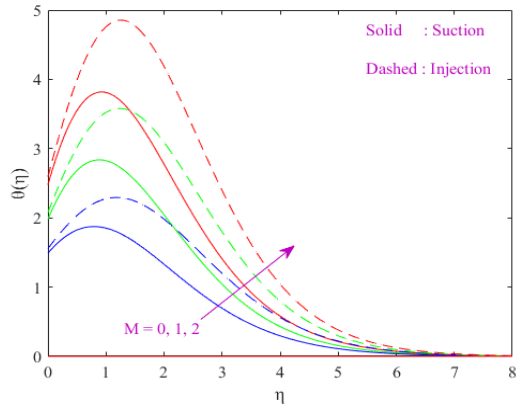

Fig. 5. Temperature $\theta(\eta)$ related to η for unlike facts of Magnetic restriction M .

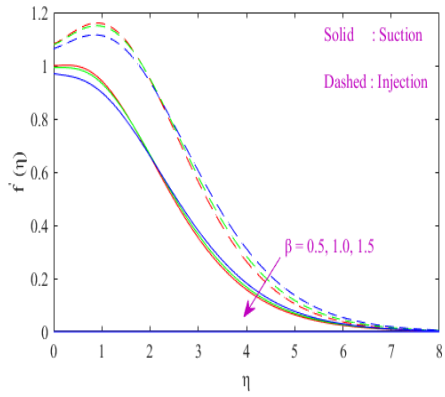

Fig. 6. Velocity profiles $f'(\eta)$ against η for unlike values of Casson fluid restriction β .

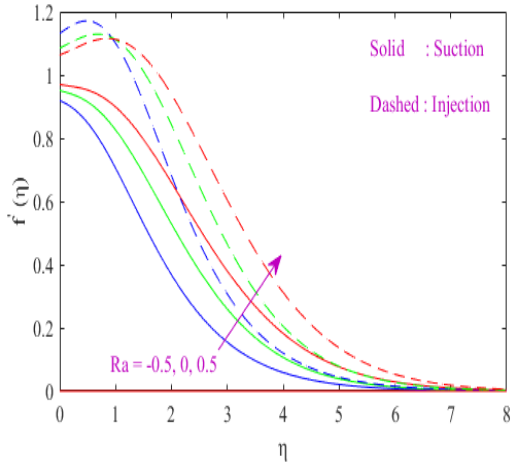

Fig. 7. Velocity $f'(\eta)$ against η for unlike values of radiation restriction Ra .

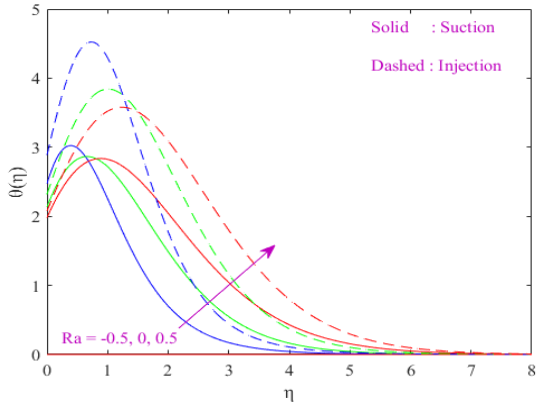

Fig. 8. Temperature related to η for unlike facts of radiation restriction Ra .

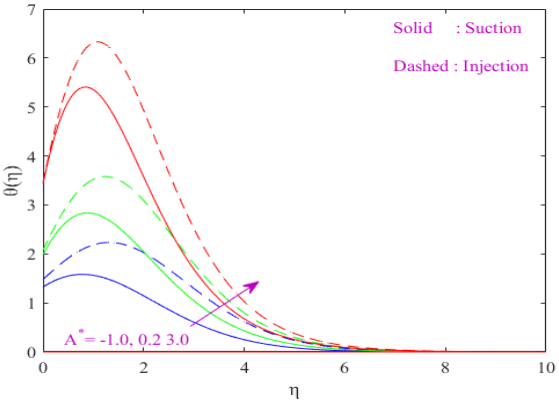

Fig. 9. Temperature $\theta(\eta)$ related to η for unlike facts of non-unchanging heat sink/source restriction $A*$.

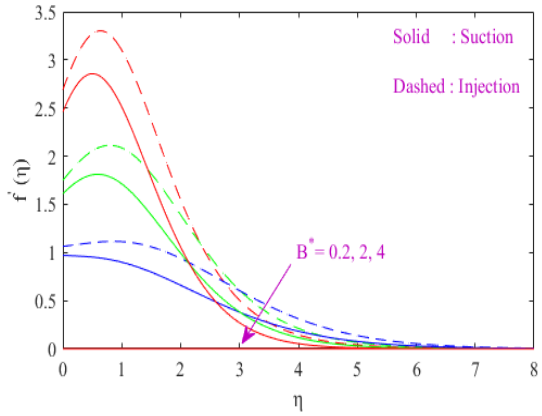

Fig. 10. Velocity against η for unlike facts of non-unchanging heat sink/source restriction $B*$.

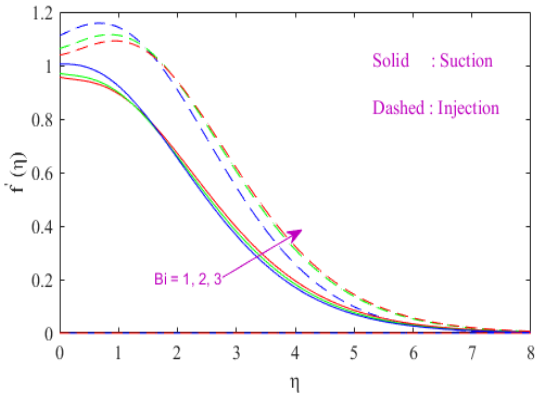

Fig. 11. Velocity against η for unlike facts of Biot Numeral.

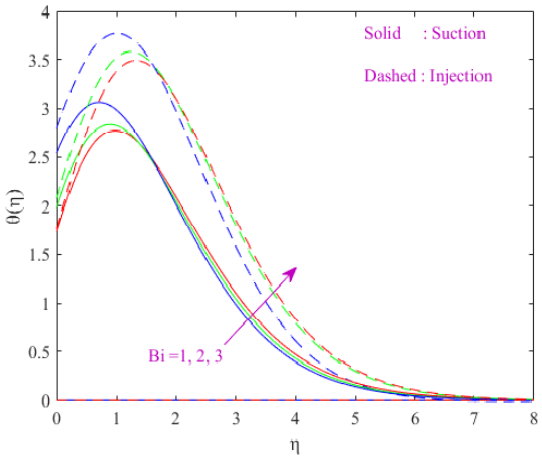

Fig. 12. Temperature profiles $\theta(\eta)$ related to η for unlike facts of Biot Numeral.

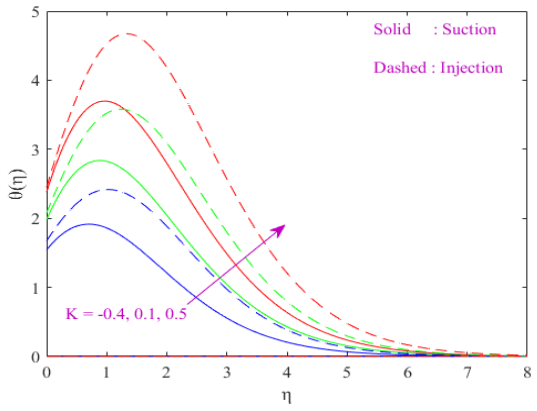

Fig. 13. Temperature related to η for unlike facts of Permeability restriction K.

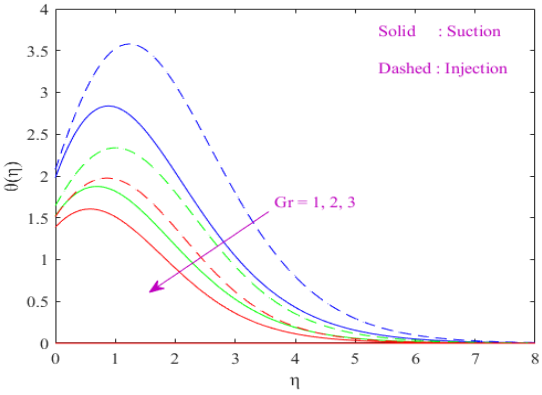

Fig. 14. Temperature $\theta(\eta)$ related to η for unlike facts of Grashof numeral Gr.

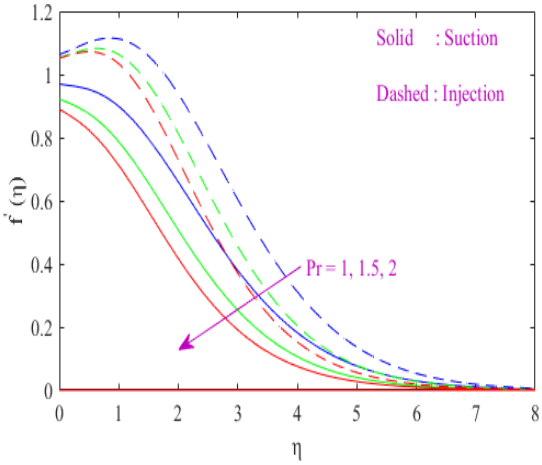

Fig. 15. Velocity profiles $f'(\eta)$ against η for unlike facts of Prandtl numeral Pr.

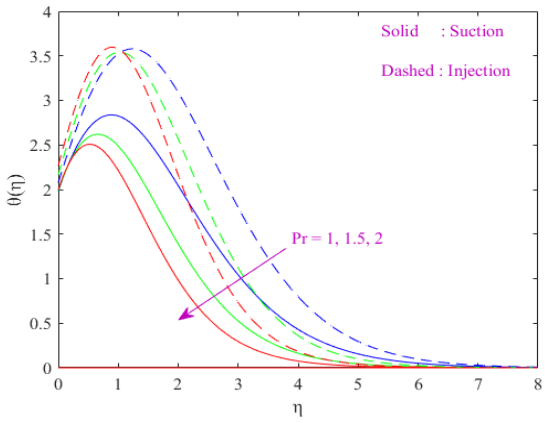

Fig. 16. Temperature $\theta(\eta)$ related to η for unlike facts of Prandtl numeral Pr.

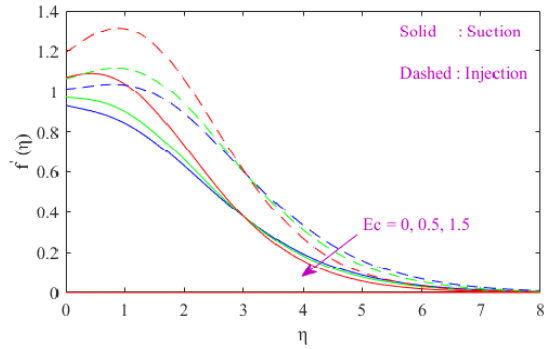

Fig. 17. Velocity profiles $f'(\eta)$ against η for unlike values of Eckert numeral Ec.

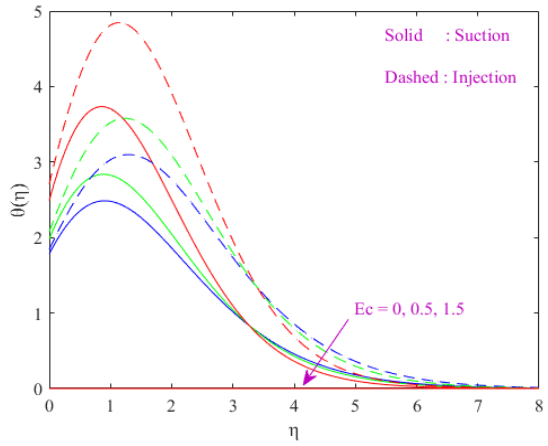

Fig. 18. Temperature $\theta(\eta)$ related to η for unlike facts of Eckert numeral Ec.

Table 1. Encouragement of numerous non-dimensional leading restrictions on friction factor C_{f_x}.

	C_{f_x}	
	Suction	Injection
$M = 0$	-0.044724	0.233124
$M = 1$	-0.090954	0.190482
$M = 2$	-0.125655	0.147111
$Bi = 1$	0.016017	0.333147
$Bi = 2$	-0.090954	0.190482
$Bi = 3$	-0.131463	0.116598
$Pr = 1$	-0.090954	0.190482
$Pr = 1.5$	-0.233811	0.161178
$Pr = 2$	-0.330780	0.155508
$K = -0.4$	0.208824	0.555741
$K = 0.1$	-0.090954	0.190482
$K = 0.5$	-0.224790	0.017085
$Gr = 1$	-0.090954	0.190482
$Gr = 2$	0.255420	0.616539
$Gr = 3$	0.616470	1.036947
$A^* = -1$	-0.586719	-0.256689
$A^* = 0.2$	-0.090954	0.190482
$A^* = 3$	0.773559	1.020012
$B^* = 0.2$	-0.090954	0.190482
$B^* = 2$	1.830693	2.250153
$B^* = 4$	4.381713	5.070933
$Ec = 0$	-0.213570	0.037455
$Ec = 0.5$	-0.090954	0.190482
$Ec = 1.5$	0.208284	0.576030

Table 2. Encouragement of numerous non-dimensional leading restrictions on Nusselt numeral (Nu).

	Nu	
	Suction	Injection
$M = 0$	-1.468635	-1.668135
$M = 1$	-2.943000	-3.230670
$M = 2$	-4.427543	-4.777658
$Bi = 1$	-2.303715	-2.695850
$Bi = 2$	-2.943000	-3.230670
$Bi = 3$	-3.270000	-3.413700
$Pr = 1$	-2.943000	-3.230670
$Pr = 1.5$	-2.958000	-3.499335
$Pr = 2$	-2.997000	-3.796620
$K = -0.4$	-1.627560	-2.016006
$K = 0.1$	-2.943000	-3.230670

$K = 0.5$	-4.138625	-4.350125
$Gr = 1$	-2.943000	-3.230670
$Gr = 2$	-1.567650	-1.931400
$Gr = 3$	-1.163250	-1.545375
$A^* = -1$	-0.975000	-1.432875
$A^* = 0.2$	-2.943000	-3.230670
$A^* = 3$	-7.297877	-7.384950
$B^* = 0.2$	-2.943000	-3.230670
$B^* = 2$	-14.925990	-15.555090
$B^* = 4$	-39.677895	-41.822895
$Ec = 0$	-2.348295	-2.529945
$Ec = 0.5$	-2.943000	-3.230670
$Ec = 1.5$	-4.466169	-5.119719

6. Conclusions

This paper provides a concurrent explanation for a two-dimensional laminal stream of Casson fluid that conducts electricity through a vertical surface in the presence of a heat sink/source. The effect of multiple non-dimensional limits on velocity and thermal field is intentional and is given via graphs. The belongings of physical restrictions on friction factors and Nusselt values are analyzed and shown through tables in the case of suction and injection. The results findings are brief as follows.

- Figs. 3 and 4 display that Extend magnetic field limitations result in reduced velocity and improved temperature distribution.
- Figs. 7, 11 and 8, 12 show that Radiation limitation and Biot number assistance to improve field velocity and temperature field distribution in suction and injection.
- In Figs. 2, 15, 17 and 3, 16, 18 notice that Rise in the suction/injection restriction, Prandtl numeral and Eckert numeral, diminutions the velocity arena and circulation of temperature in both injection and suction cases.
- Nusselt numeral is lessened for an appreciation of magnetic field, Biot numeral, Prandtl numeral, Permeability restriction, Eckert numeral and non-unchanging heat sink/source restrictions (A^*, B^*) and increased for Grashof numeral.Friction factor is an growing function of Grashof numeral, Eckert numeral and non-unchanging heat sink/source restrictions (A^*, B^*) and decreased for magnetic field, Biot numeral, Prandtl numeral, Permeability restriction.

References

[1] Hayat, T., and Alsaedi, A. On thermal radiation and joule heating effects in mhd flow of an oldroyd-b fluid with thermophoresis. Arabian Journal for Science and Engineering 36, 6 (2011), 1113-24.

[2] Zheng, L.-C., Jin, X., Zhang, X.-X., and Zhang, J.-H. Unsteady heat and mass transfer in mhd flow over an oscillatory stretching surface with soret and dufour effects. ActaMechanicaSinica 29, 5 (2013), 667-75.

[3] Khalid, A., Khan, I., Khan, A., and Shafie, S. Unsteady mhd free convection flow of casson fluid past over an oscillating vertical plate embedded in a porous medium. Engineering Science and Technology, an International Journal 18, 3 (2015), 309-17.

[4] Reddy, M. G. Unsteady radiative-convective boundary-layer flow of a casson fluid with variable thermal conductivity. Journal of Engineering Physics and Thermophysics 88, 1 (2015), 240-51.

[5] Hayat, T., Asad, S., and Alsaedi, A. Non-uniform heat source/sink and thermal radiation effects on the stretched flow of cylinder in a thermally stratified medium. J. Appl. Fluid Mech. 10, 3 (2016), 915-24.

[6] Kataria, H. R., and Patel, H. R. Soret and heat generation effects on mhdcasson fluid flow past an oscillating vertical plate embedded through porous medium.

Alexandria Engineering Journal 55, 3 (2016), 2125-37.

[7] Kataria, H. R., and Patel, H. R. Radiation and chemical reaction effects on mhdcasson fluid flow past an oscillating vertical plate embedded in porous medium. Alexandria Engineering Journal 55, 1 (2016), 583-95.

[8] Sandeep, N., Koriko, O. K., and Animasaun, I. L. Modified kinematic viscosity model for 3d-casson fluid flow within boundary layer formed on a surface at absolute zero. Journal of Molecular Liquids 221 (2016), 1197-206.

[9] Raju, C., and Sandeep, N. Heat and mass transfer in mhd non-newtonian bio-convection flow over a rotating cone/plate with cross diffusion. Journal of molecular liquids 215 (2016), 115-26.

[10] Naramgari, S., and Sulochana, C. Mhd flow over a permeable stretching/shrinking sheet of a nanofluid with suction/injection. Alexandria Engineering Journal 55, 2 (2016), 819-27.

[11] Ahmad, K., Hanouf, Z., and Ishak, A. Mhdcassonnanofluid flow past a wedge with newtonian heating. The European Physical Journal Plus 132, 2 (2017), 1-11.

[12] Arifuzzaman, S., Hossain, K. E., Roy, R., Islam, M., Akter, S., Khan, M., et al. Chemically reactive viscoelastic fluid flow in presence of nano particle through porous stretching sheet. Frontiers in Heat and Mass Transfer (FHMT) 9, 1 (2017).

[13] Baag, S., Mishra, S., Dash, G., and Acharya, M. Numerical investigation on mhdmicropolar fluid flow toward a stagnation point on a vertical surface with heat source and chemical reaction. Journal of King Saud University-Engineering Sciences 29, 1 (2017), 75-83.

[14] Kumaran, G., and Sandeep, N. Thermophoresis and brownian moment effects on parabolic flow of mhdcasson and williamsonfluids with cross diffusion. Journal of Molecular Liquids 233 (2017), 262-9.

[15] Khan, M. I., Waqas, M., Hayat, T., and Alsaedi, A. A comparative study of casson fluid with homogeneous-heterogeneous reactions. Journal of colloid and interface science 498 (2017), 85-90.

[16] Tamoor, M., Waqas, M., Khan, M. I., Alsaedi, A., and Hayat, T. Magnetohydrodynamic flow of casson fluid over a stretching cylinder. Results in physics 7 (2017), 498-502.

[17] Hussanan, A., Salleh, M. Z., Khan, I., and Shafie, S. Analytical solution for suction and injection flow of a viscoplasticcasson fluid past a stretching surface in the presence of viscous dissipation. Neural computing and applications 29, 12 (2018), 1507-15.

[18] Ullah, I., Shafie, S., Khan, I., and Hsiao, K. L. Brownian diffusion and thermophoresis mechanisms in casson fluid over a moving wedge. Results in Physics 9 (2018), 183-94.

[19] Kumar, A., Sugunamma, V., and Sandeep, N. Impact of non-linear radiation on mhd non-aligned stagnation point flow of micropolar fluid over a convective surface. Journal of Non-Equilibrium Thermodynamics 43, 4 (2018), 327-45.

[20] Mohyud-Din, S. T., Usman, M., Wang, W., and Hamid, M. A study of heat transfer analysis for squeezing flow of a casson fluid via differential transform method. Neural Computing and Applications 30, 10 (2018), 3253-64.

[21] Animasaun, I., Koriko, O., Adegbie, K., Babatunde, H., Ibraheem, R., Sandeep, N., and Mahanthesh, B. Comparative analysis between 36 nm and 47 nm alumina–water nanofluid flows in the presence of hall effect. Journal of Thermal Analysis and Calorimetry 135, 2 (2019), 873-86.

[22] Dogonchi, A., et al. Heat transfer by natural convection of fe3o4-water nanofluid in an annulus between a wavy circular cylinder and a rhombus. International Journal of Heat and Mass Transfer 130 (2019), 320-32.

[23] Dogonchi, A., Ismael, M. A., Chamkha, A. J., and Ganji, D. Numerical analysis of natural convection of cu–water nanofluid filling triangular cavity with semicircular bottom wall. Journal of Thermal Analysis and Calorimetry 135, 6 (2019), 3485-97.

[24] Dogonchi, A. S., Armaghani, T., Chamkha, A. J., and Ganji, D. Natural convection analysis in a cavity with an inclined elliptical heater subject to shape factor of nanoparticles and magnetic field. Arabian Journal for Science and Engineering 44, 9 (2019), 7919-31.

[25] Dogonchi, A., Sheremet, M., Ganji, D., and Pop, I. Free convection of copper–water nanofluid in a porous gap between hot rectangular cylinder and cold circular cylinder under the effect of inclined magnetic field. Journal of Thermal Analysis and Calorimetry 135, 2 (2019), 1171-84.

[26] Kumar, K. A., Ramadevi, B., Sugunamma, V., and Reddy, J. R. Heat transfer characteristics on mhdpowell-eyring fluid flow across a shrinking wedge with non-uniform heat source/sink. Journal of Mechanical Engineering and Sciences 13, 1 (2019), 4558-74.

[27] Kumar, K. A., Reddy, J. R., Sugunamma, V., and Sandeep, N. Simultaneous solutions for mhd flow of williamson fluid over a curved sheet with nonuniform heat source/sink. Heat Transfer Research 50, 6 (2019).

[28] Kumar, K. A., Reddy, J. R., Sugunamma, V., and Sandeep, N. Mhd flow of chemically reacting williamson fluid over a curved/flat surface with variable heat source/sink. International Journal of Fluid Mechanics Research 46, 5 (2019).

[29] Kumar, K. A., Sugunamma, V., and Sandeep, N. A non-fourier heat flux model for magnetohydrodynamicmicropolar liquid flow across a coagulated sheet. Heat Transfer-Asian Research 48, 7 (2019), 2819-43.

[30] Kumar, K. A., Sugunamma, V., and Sandeep, N. Influence of viscous dissipation on mhd flow of micropolar fluid over a slendering stretching surface with modified heat flux model. Journal of Thermal Analysis and Calorimetry 139, 6 (2020), 3661-74.

[31] Reza-E-Rabbi, S., Arifuzzaman, S., Sarkar, T., Khan, M. S., and Ahmmed, S. F. Explicit finite difference analysis of an unsteady mhd flow of a chemically reacting casson fluid past a stretching sheet with brownian motion and thermophoresis effects. Journal of King Saud University-Science 32, 1 (2020), 690-701.

[32] Agrawal, P., Dadheech, P. K., Jat, R., Baleanu, D., and Purohit, S. D. Radiativemhdhybridnanofluids flow over a permeable stretching surface with heat source/sink embedded in porous medium. International Journal of Numerical Methods for Heat & Fluid Flow (2021).

[33] Agrawal, P., Dadheech, P. K., Jat, R., Nisar, K. S., Bohra, M., and Purohit, S. D. Magneto marangoni flow of γ- al2o3 nanofluidswith thermal radiation and heat source/sink effects over a stretching surface embedded in porous medium. Case Studies in Thermal Engineering 23 (2021), 100802.

[34] Mathur, P., Mishra, S., Purohit, S., and Bohra, M. Entropy generation in a micropolar fluid past an inclined channel with velocity slip and heat flux conditions: Variation parameter method. Heat Transfer 50, 7 (2021), 7425-39.

[35] Dadheech, P. K., Agrawal, P., Sharma, A., Dadheech, A., Al-Mdallal, Q., and Purohit, S. D. Entropy analysis for radiative inclined mhd slip flow with heat source in porous medium for two different fluids. Case Studies in Thermal Engineering 28 (2021), 101491.